The p12 subunit of human polymerase δ uses an atypical PIP box for molecular recognition of proliferating cell nuclear antigen (PCNA)

Amaia Gonzalez-Magaña[‡], Alain Ibáñez de Opakua[‡1], Miguel Romano-Moreno[‡], Javier Murciano-Calles[§], Nekane Merino[‡], Irene Luque[§], Adriana L. Rojas[‡], Silvia Onesti[¶], Francisco J. Blanco[‡||2], and Alfredo De Biasio[¶**3]

From the [‡]CIC bioGUNE, Parque Tecnológico de Bizkaia Edificio 800, 48160 Derio, Spain, the [§]Department of Physical Chemistry and Institute of Biotechnology, Universidad de Granada, Granada 18071, Spain, the [¶]Structural Biology Laboratory, Elettra-Sincrotrone Trieste S.C.p.A., Trieste 34149, Italy, [||]IKERBASQUE, Basque Foundation for Science, 48013 Bilbao, Spain, and the [**]Leicester Institute of Structural & Chemical Biology and Department of Molecular & Cell Biology, University of Leicester, Leicester LE1 7HB, United Kingdom

Edited by Patrick Sung

Human DNA polymerase δ is essential for DNA replication and acts in conjunction with the processivity factor proliferating cell nuclear antigen (PCNA). In addition to its catalytic subunit (p125), pol δ comprises three regulatory subunits (p50, p68, and p12). PCNA interacts with all of these subunits, but only the interaction with p68 has been structurally characterized. Here, we report solution NMR–, isothermal calorimetry–, and X-ray crystallography–based analyses of the p12–PCNA interaction, which takes part in the modulation of the rate and fidelity of DNA synthesis by pol δ. We show that p12 binds with micromolar affinity to the classical PIP-binding pocket of PCNA via a highly atypical PIP box located at the p12 N terminus. Unlike the canonical PIP box of p68, the PIP box of p12 lacks the conserved glutamine; binds through a 2-fork plug made of an isoleucine and a tyrosine residue at +3 and +8 positions, respectively; and is stabilized by an aspartate at +6 position, which creates a network of intramolecular hydrogen bonds. These findings add to growing evidence that PCNA can bind a diverse range of protein sequences that may be broadly grouped as PIP-like motifs as has been previously suggested.

Three eukaryotic DNA polymerases (pols),[4] α, δ, and ε, participate in chromosomal DNA replication (1), with the latter two possessing the proofreading exonuclease activity required to replicate DNA with high fidelity. Human pol δ consists of a catalytic subunit (p125, harboring the polymerase and exonuclease activities), associated with three regulatory subunits (p50, p68, also known as p66, and p12) needed for optimal holoenzyme function (2, 3), and there is evidence of different context-specific subassemblies of pol δ *in vivo* (3–5). In particular, DNA damage or replication stress triggers the degradation of p12, a 12-kDa polypeptide of unknown structure, resulting in the formation of a three-subunit enzyme with an increased capacity for proofreading (3, 4, 6). The processive activity of pol δ in DNA replication (*i.e.* the ability of the polymerase to synthesize hundreds of bp without detaching from the template) is conferred by its association with the sliding clamp PCNA, a ring-shaped homotrimer that encircles and slides on DNA (6–8).

Structurally, little is known on how the four subunits of mammalian pol δ interact with each other and PCNA. The p125 catalytic subunit and the p50 subunit form a tight heterodimer, which constitutes the core enzyme (9). Biochemical analysis showed that the p68 subunit is attached to the core enzyme via an interaction between its N-terminal domain and p50, whereas p12 bridges the p125 and p50 subunits (10, 11). However, structural information is limited to the p50–p68 interaction only (12). The p125 subunit, which is composed of a catalytic domain and a C-terminal domain containing an iron–sulfur cluster (13), has been reported to directly interact with PCNA (14, 15), but the p125–PCNA complex showed negligible processivity *in vitro* (16), suggesting that the interaction is weak. Similarly, the p50–PCNA interaction, if any, is very weak (10, 17). On the other hand, the interactions between the p68 and p12 subunits and PCNA seem tighter (10, 18), and especially p68 is critical for pol δ–PCNA processivity (16). For both p68 and p12, examination of reconstituted holoenzymes in

---

[4] The abbreviations used are: pol, polymerase; PCNA, proliferating cell nuclear antigen; PDB, Protein Data Bank; CSP, chemical shift perturbation; ITC, isothermal titration calorimetry; IDCL, interdomain connector loop; TROSY, transverse relaxation-optimized spectroscopy.
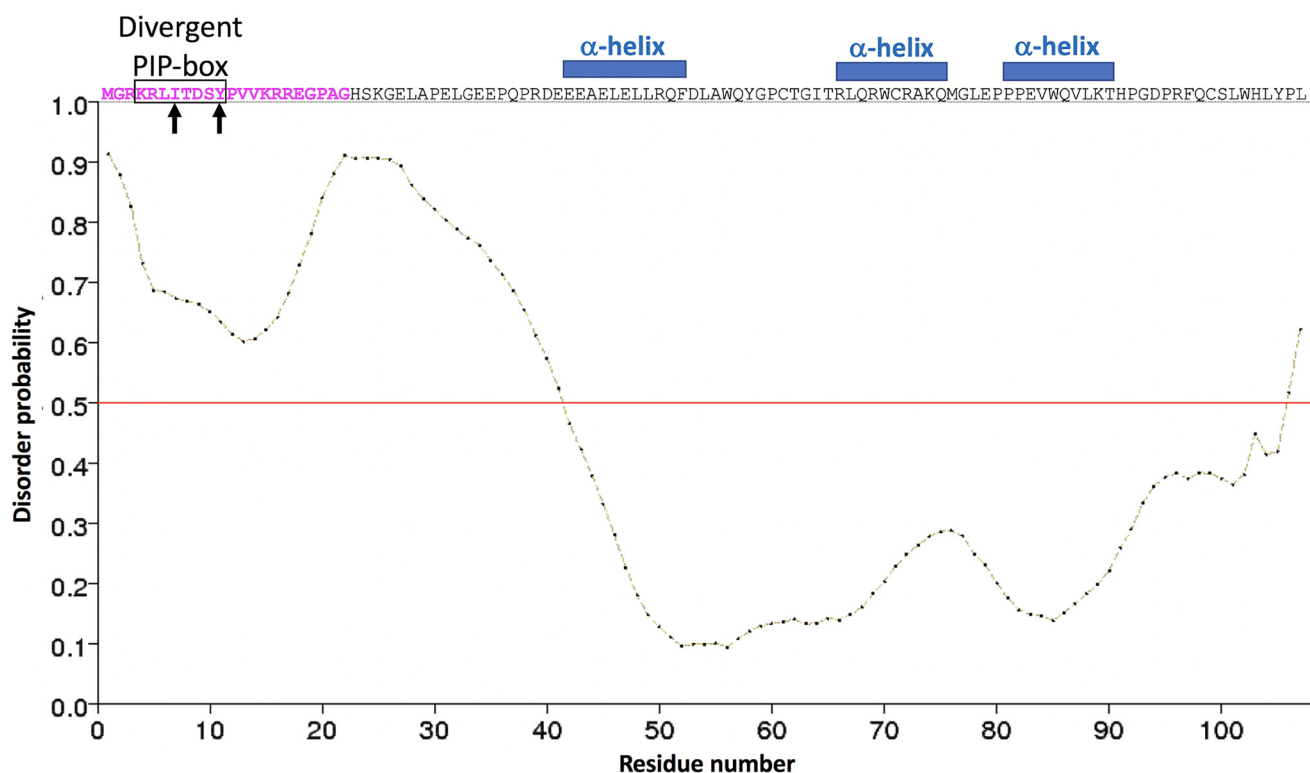
SASBMB

J. Biol. Chem. (2019) 294(11) 3947–3956 **3947**

Figure 1. Amino acid sequence of p12 together with disorder and secondary structure predictions. Residues encompassing the peptide used for crystallization and biophysical characterization (p12$^{1-19}$) with PCNA are indicated in *bold pink characters*, and those belonging to the divergent PCNA interacting motif are *boxed*. The consensus residues in the PIP-like motif are indicated by *arrows*. The *solid line* shows the disorder prediction by the PrDOS server (51), and the *red line* shows the threshold of 0.5. Secondary structure elements (helices predicted by JPred4 (52)) are indicated *above* the sequence.

which the PCNA-binding motifs (the PIP box) have been mutated or inactivated has been performed (3, 10, 19), and it was found that both PIP boxes were necessary for optimal pol δ activity. The PIP-box strict consensus sequence is Q*XXhXXaa*, where *h* is a hydrophobic, *a* is an aromatic, and *X* is any residue. The crystal structure of a peptide spanning the canonical PIP-box of p68 (^{456}QVS$\underline{I}$TG$\underline{FF}^{462}$) bound to PCNA has been determined, showing the PIP box interacting through the prototypical molecular surface observed in other PCNA-interacting partners (20). The p68 PIP box is located at the C-terminal region, which is predicted to be disordered (Fig. S1). Upon binding, the PIP box forms a 3_{10} helix, and the conserved hydrophobic trident inserts into a hydrophobic patch located between the N- and C-terminal domains of the PCNA protomer, whereas the glutamine binds in the so called "Q pocket" (20). By contrast, the PCNA-binding site of p12 is located in an N-terminal region (10), also predicted to be intrinsically disordered, and the proposed PIP box, whereas highly conserved in mammals, is noncanonical (^{4}KRL$\underline{I}$TD$\underline{SY}^{11}$; Fig. 1). Mutation of p12 residues Ile^7, Ser^{10}, and Tyr^{11} in the putative PIP box results in defective binding of recombinant pol δ to PCNA, as well as in reduced pol δ processivity (10).

Because the p12 PIP box significantly diverges from the strict PIP-box consensus sequence, we wondered whether it may encode for a novel PCNA-binding motif with exclusive structural specificities. We therefore analyzed the p12–PCNA interaction by crystallography, NMR, and isothermal calorimetry. Our data shows that a 19-residue p12 peptide containing the PCNA-binding site recognizes PCNA via its divergent PIP box, which adopts a characteristic 3_{10} helical fold. In the p12 PIP

box, the absence of the glutamine and the aromatic residue at +7 position and their associated stabilizing intermolecular interactions is counterbalanced by an intramolecular hydrogen-bonding network centered on the aspartate at +6 position, which stabilizes the 3_{10} helical conformation. Based on our data, p12 and p68 subunits contribute to the molecular recognition of PCNA by pol δ with different structural specificities and affinities.

Surprisingly, we have found that the affinity of the p12–PCNA interaction is higher than that measured for the canonical PIP box of the human DNA helicase RecQ5. These results reinforce the emerging idea of the existence of a broader class of PCNA-interacting sequences, which may be called "PIP-like" motifs (21).

Results

NMR and ITC analysis of the p12–PCNA interaction

We first observed and characterized the interaction of PCNA with p12$^{1-19}$ by solution NMR. ^{2}H-^{15}N–Labeled PCNA was titrated with unlabeled p12 peptide, and the chemical shift perturbations of PCNA backbone amide signals were analyzed (Fig. 2*A*). We identified two groups of perturbed residues: those whose signals gradually shift along the titration, implying a fast exchange regime on the NMR time scale (Fig. 2*B*), and those residues whose signals broaden and disappear (because of signal attenuation below the noise level or untraceable shifting), indicating an intermediate exchange regime. When plotting the chemical shift perturbations (CSPs) along the PCNA sequence
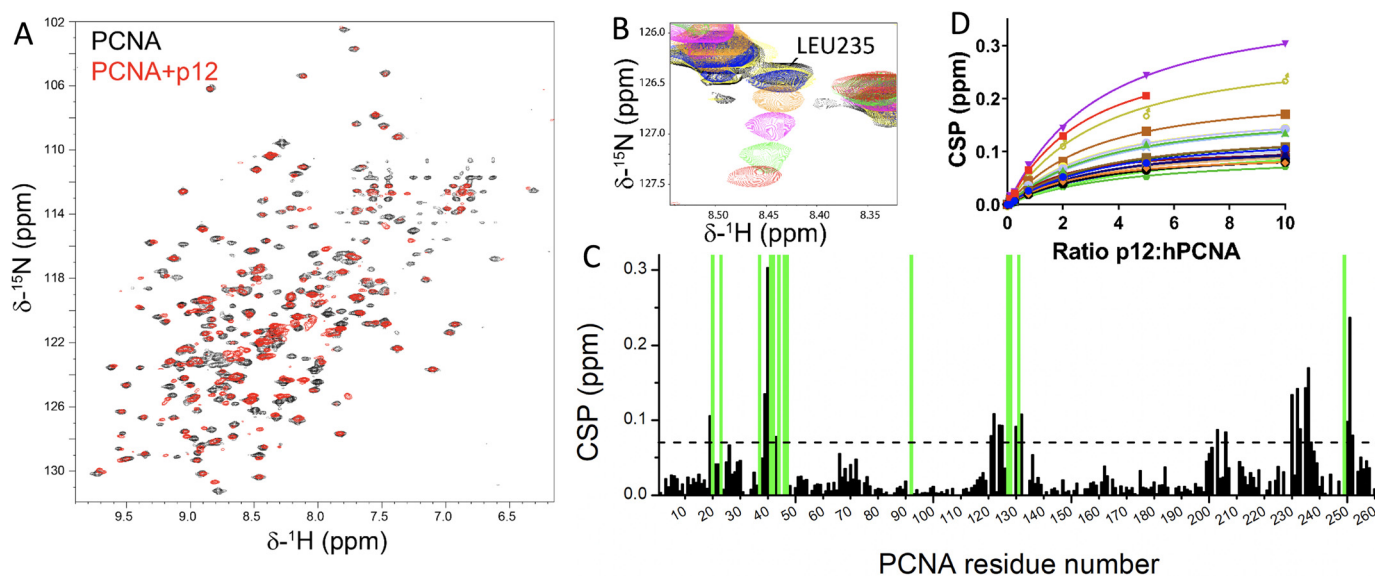
Figure 2. NMR analysis of the p12 peptide interaction with PCNA. *A*, superposition of ^1H-^{15}N TROSY spectra of 51 μM PCNA in the absence (*black*) and presence (*red*) of a 10-fold molar excess of p12$^{1-19}$ peptide. Spectra were acquired at 35 °C in PBS, pH 7.0, 1 mM DTT. *B*, region of the NMR spectra of PCNA in the presence of increasing amounts of p12 peptide (from *black* to *red*) showing the titration of Leu^{235} signal. *C*, CSPs of PCNA backbone amide ^1H and ^{15}N NMR resonances induced by p12$^{1-19}$. The *dashed line* indicates the average plus one standard deviation. The *green bars* indicate the positions of residues that disappear upon peptide addition. *D*, chemical shift perturbation of the amide signal of residues with CSP larger than the average plus one standard deviation at different p12:PCNA ratios. The *symbols* correspond to the experimental data, and the *lines* correspond to the best fits to a model of one set of identical binding sites.

(Fig. 2C), a similar pattern as for p21 binding is observed (22), suggesting a similar mode of binding. The titration of the signals from those residues with CSP values larger than the average plus one standard deviation yielded an average dissociation constant of 130 $\pm$ 30 μM at 35 °C (Fig. 2D).

Isothermal titration calorimetry (ITC) measurements could be fitted well to a model of independent p12 peptide binding to equivalent sites in the PCNA trimer ($n = 0.87 \pm 0.02$), with a dissociation constant of 38 $\pm$ 4 μM at 25 °C (Fig. 3). Thus, three p12 peptides bind to the three equivalent PCNA protomers, in agreement with the NMR spectra, which show a single set of signals along the titration. The enthalpic term is negative ($\Delta H = -8.1 \pm 0.3$ kcal/mol) and is the driving force for the favorable Gibbs free energy, whereas the entropic term is unfavorable ($-T\Delta S = 2.1 \pm 0.4$ kcal/mol) and is in line with a loss of conformational freedom of the p12 peptide upon binding to PCNA.

Crystal structure of the p12–PCNA complex

Crystals of PCNA bound to the p12 peptide diffracted to 2.1 Å resolution (Table 1), and the Fourier difference map calculated after placing and refining the PCNA ring alone in the asymmetric unit showed peaks of positive electron density across all three canonical PIP-box sites on PCNA, arising from three bound p12 peptides (Fig. S2). The structure of the PCNA ring is virtually identical to the previously determined structure of native human PCNA (PDB code 1VYM (23); root mean square deviation of C$^\alpha$ = 0.67 Å). The three p12 peptides in the three PIP-box sites have nearly identical conformations and occupancies. Small differences were observed in the length of the modeled peptides according to their visibility in the electron density map, and vary from 12 (Lys^4–Lys^{15}) to 13 residues (Arg^3–Lys^{15}). p12 residues 7–10 adopt a 3$_{10}$ helical conforma-

tion (Fig. 4A), stabilized by an intramolecular hydrogen-bonding network in which the side chain carboxyl group and main chain nitrogen atom of Asp^9 form hydrogen bonds with the main chain nitrogen and oxygen atoms of Leu^6, respectively, whereas the main chain nitrogen atoms of both Ser^{10} and Tyr^{11} interact with the carbonyl oxygen of Ile^7 (Fig. 4B). The 3$_{10}$ helix inserts into the hydrophobic cavity under the interdomain connector loop (IDCL) of PCNA (Fig. 4, *B* and *C*). The side chains of Ile^7 and Tyr^{11} insert into the hydrophobic cavity, where the former is fully buried in the pocket lined with hydrophobic side chains of Met^{40}, Leu^{47}, and Tyr^{250}, and the latter is caged by the side chains of Ile^{128}, Pro^{234}, and Tyr^{250}. Differently from the canonical PIP box, the p12 PIP box lacks the terminal glutamine and an aromatic residue at +7 position and thus lacks the stabilizing hydrophobic interactions mediated by those residues (20). The p12–PCNA interaction is further stabilized by four intermolecular hydrogen bonds involving the backbone groups of p12 residues Ile^7, Pro^{12}, Val^{14}, and Lys^{15} and those of PCNA residues His^{44}, Gln^{125}, and Gly^{127} and one salt bridge between p12 residue Arg^5 and residue Asp^{232} on one exposed loop of PCNA (Fig. 4C). Notably, p12 lacks the stabilizing interactions established with the C terminus of PCNA observed in the p68–PCNA structure (20) (Fig. 4D).

Comparison of p12 and RecQ5 interactions with PCNA

We have also characterized by NMR the interaction of PCNA with a peptide derived from the RecQ5 helicase (Fig. 5A). RecQ5 plays an important role in the resolution between replication and transcription machineries (24), partly by a direct interaction with PCNA mediated by a C-terminal canonical PIP box (^{964}QNLIRHFF^{971}) (25). The RecQ5 PIP box drew our attention because the residues preceding the aromatic residues are basic, instead of the more common neutral or acidic ones.
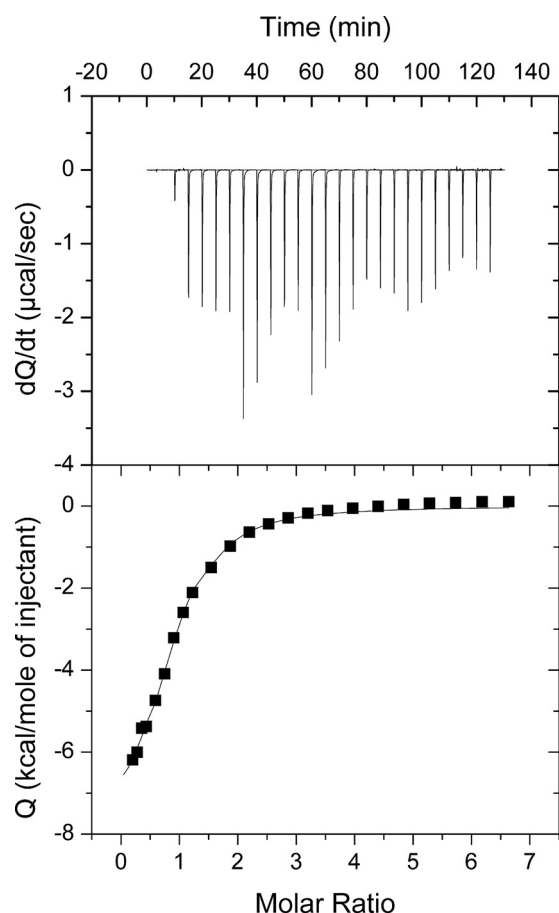
Figure 3. Isothermal calorimetric titration of PCNA with p12 peptide. The *upper panel* represents the heat effect associated with the variable volume peptide injection, and the *lower panel* represents the ligand concentration dependence of the heat released upon binding, after normalization and correction for the heat of dilution. The molar ratio is that of p12:PCNA protomer. The *symbols* correspond to the experimental data, and the *continuous line* corresponds to the best fit to a model of one set of identical binding sites.

Table 1
Crystallographic statistics

PDB code	6HVO
Data collection	
Space group	P212121
Cell dimensions	
a, b, c (Å)	71.97, 83.89, 154.98
α, β, γ (°)	90.0, 90.0, 90.0
Resolution (Å)	77.5–2.1 (2.16–2.10)
R_{meas}	0.17 (2.84)
R_{merge}	0.17 (2.9)
$CC_{1/2}$ (%)	99.6 (44.7)
$I/\sigma I$	10.7 (1.3)
Completeness (%)	100.0 (100.0)
Redundancy	12.9 (13.2)
Refinement	
Resolution (Å)	73.9–2.1
No. reflections	55,825
R_{work}/R_{free}	19.5/24.4
No. atoms	
Protein	5,928
Ligand/ion	320/35
Water	243
B-factors	
Protein	50.22
Ligand/ion	61.40/65.64
Water	51.61
Root mean square deviations	
Bond lengths (Å)	0.009
Bond angles (°)	1.49

The NMR titration of ^{2}H-^{15}N–labeled PCNA with unlabeled RecQ5 peptide shows a pattern of CSP similar to that of p12 (Fig. 5*B*), but a higher peptide:PCNA ratio is necessary to approach a saturation level similar to p12 (Fig. 5*C*). Those residues with CSP values larger than the average plus one standard deviation yielded an average dissociation constant of 210 ± 50 μM at 35 °C. Surprisingly, the affinity of binding of this canonical PIP box is lower than that measured for the divergent PIP box of p12 under identical conditions (Fig. 4*C*). Our attempts to crystallize the complex formed by the RecQ5 peptide and PCNA were unsuccessful, but mapping the CSPs on the surface of PCNA shows that the RecQ5-binding site is located on the canonical PIP-box pocket of PCNA and involves only a limited portion of the IDCL (Fig. 6*A*). By contrast, the same mapping for p12 form a continuous surface centered on the PIP box–binding site and IDCL (Fig. 6*B*), consistent with the p12–PCNA crystallographic interface and the higher affinity than RecQ5.

Discussion

Role of p12 subunit in the molecular recognition of PCNA by pol δ

Our work reveals that the p12 and p68 subunits of pol δ interact differently with PCNA. Our crystal structure shows that, unlike p68, p12 recognizes PCNA through a highly divergent PIP box that lacks the terminal glutamine as well as the aromatic residue at +7 position in the consensus sequence. The PIP box of p12 binds the classical hydrophobic pocket on PCNA, through a 2-fork plug made of an isoleucine and a tyrosine residue at +3 and +8 positions, respectively. In the absence of the mentioned key consensus residues, the presence of an acidic residue at +6 position seems important to establish a network of intramolecular hydrogen bonds that stabilize the p12 peptide in the 3_{10} helical conformation. Such intramolecular stabilizing effect, mediated by an aspartate at +6 position, was also observed in the interaction of p21 PIP box with PCNA, which is the strongest interaction of a ligand with PCNA reported to date (22). Based on our ITC analysis, we estimated a stoichiometry of binding of 1:1 (peptide–PCNA protomer) and a 38 μM affinity for the p12$^{1-19}$–PCNA interaction at 25 °C, which is 2.4-fold lower than the 16 μM affinity measured for the p68 PIP box at the same temperature (20). The affinity of the full pol δ complex for PCNA encircling DNA is much higher (dissociation constant, <10 nM (26)), implying that the p125 and p50 subunits must also contribute to the formation of a tight pol δ–PCNA holoenzyme. In particular, p125 was shown to interact with PCNA via an N-terminal segment (14, 15, 27) that, based on our modeling, is buried within a structurally conserved region of the catalytic domain and therefore rather inaccessible (Fig. S3). An alternative PCNA interaction site in p125 may be located at the flexible C terminus of the catalytic domain, as observed in the crystal structure of *Pyrococcus furiosus* polymerase B bound to PCNA (28) (Fig. S3). The PCNA-binding motifs of p68 and p12 are both located in regions predicted to be disordered (Fig. 1 and Fig. S1), suggesting that flexibility is key to accommodate the two subunits on one PCNA ring, along with the bulkier p125 and p50 subunits (Fig. 7).
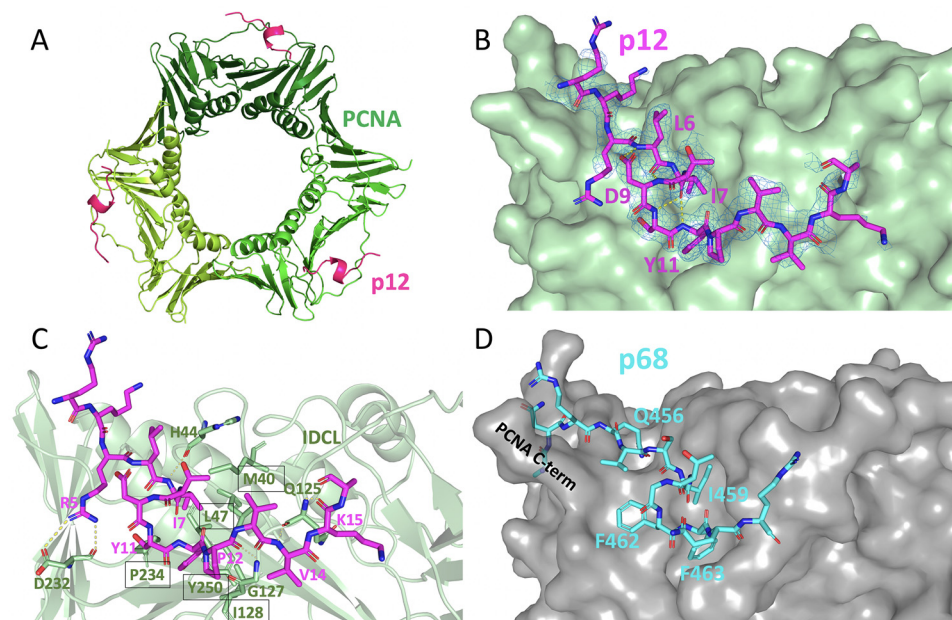
Figure 4. Crystal structure of the p12–PCNA complex and comparison with p68–PCNA structure. *A*, overall structure of trimeric human PCNA (*green*) bound to the peptide derived from p12 (p12[1–19], *magenta*). Only p12 residues 3–15 are seen in the electron density map. *B*, p12–PCNA–binding site highlighting p12 intramolecular interactions. PCNA surface is shown in *pale green*, the p12 peptide is in *magenta* with stick representation, and interactions are shown as *yellow dotted lines*. Peptide residues involved in the interactions are labeled. $2F_o − F_c$ map around the p12 peptide is shown in *blue* contoured at 1 σ. *C*, p12–PCNA–binding site highlighting p12 intermolecular interactions. PCNA is shown in *green* with ribbon representation, p12 is in *magenta* with stick representation, and interactions are shown as *yellow dotted lines*. PCNA and p12 interacting residues are labeled. Residues of PCNA involved in hydrophobic interactions are *boxed*. *D*, p68–PCNA–binding site (PDB code 1U76 ([20])). The PCNA surface is shown in *dark gray*, and p68 (residues 453–465) is in *turquoise* stick representation. The p68 PIP-box consensus residues are labeled. *C-term*, C-terminus.
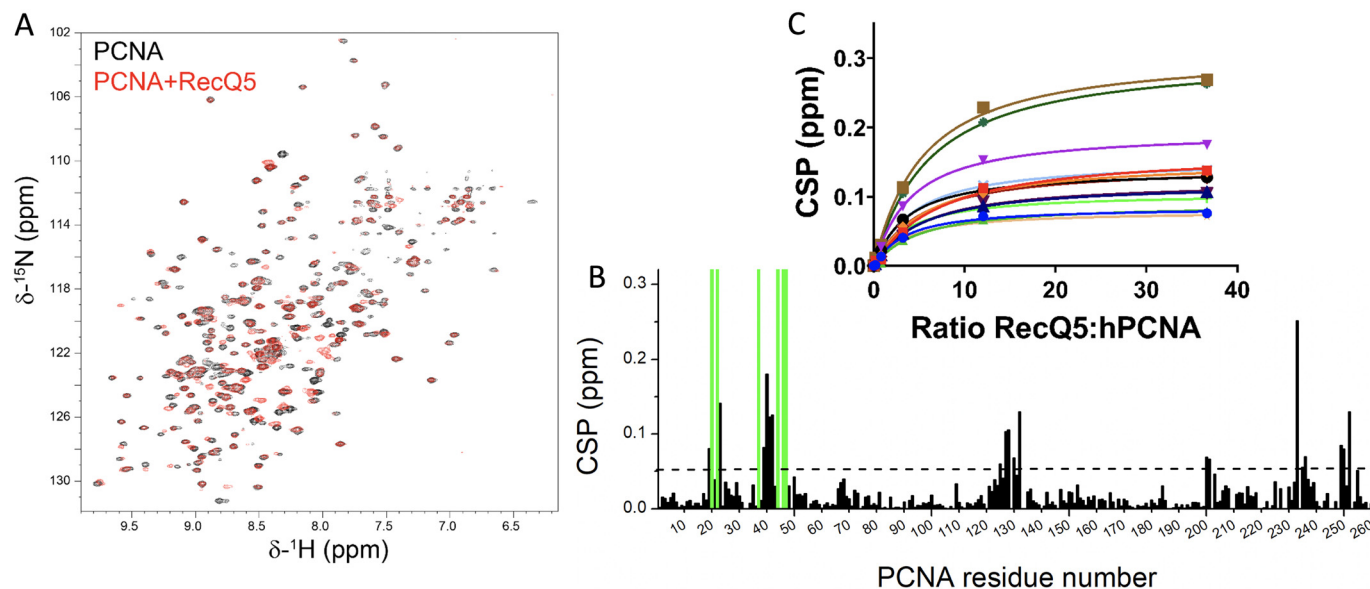

Figure 5. NMR analysis of the RecQ5 peptide interaction with PCNA. *A*, superposition of ^{1}H-^{15}N TROSY spectra of 50 μM PCNA in the absence (*black*) and presence (*red*) of a 37-fold molar excess of RecQ5 peptide. The spectra were acquired at 35 °C in PBS, pH 7.0, 1 mM DTT. *B*, CSPs of PCNA backbone amide ^{1}H and ^{15}N NMR resonances induced by RecQ5[952–979]. The *dotted line* indicates the average plus one standard deviation. The *green bars* indicate the positions of residues that disappear upon peptide addition. *C*, chemical shift perturbation of the amide signal of PCNA residues with CSPs larger than the average plus one standard deviation at different RecQ5:PCNA ratios. The *symbols* correspond to the experimental data, and the *lines* correspond to the best fit to a model of one set of identical binding sites.

Upon DNA damage or replication stress, the p12 subunit of pol δ is degraded, resulting in the formation of a three-subunit (p125–p50–p68) enzyme with enhanced proofreading capacity ([3, 5]). Thus, removal of the p12 subunit from PCNA is expected to lead to a rearrangement of the other subunits relative to each other, PCNA, and DNA, which may decrease the processivity of

the enzyme in the context of higher probability of replication mistakes. Further analyses on the architecture, dynamics, and activity of pol δ subassemblies are needed to shed light on this possibility. The degradation of p12 requires an intact ubiquitination system ([3]), and CRL4[Cdt2], a member of the Cullin family of E3 ligases, was identified as the ligase responsible for the UV-
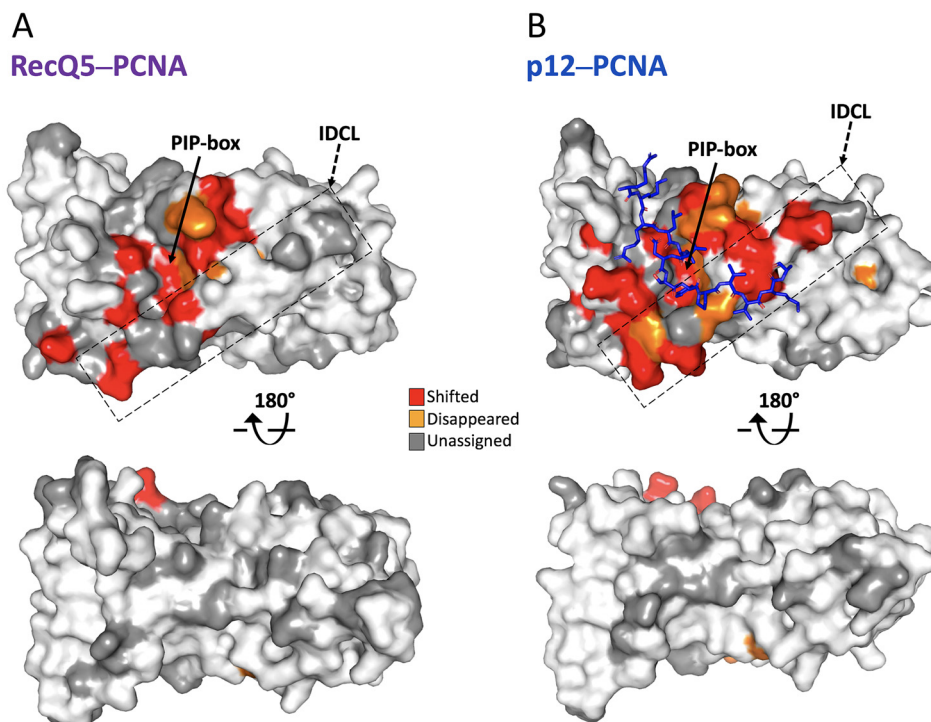
Figure 6. NMR chemical shift mapping of the RecQ5 (*A*) or p12 (*B*) interaction site on PCNA. Front and back views of one of the PCNA protomers are shown in *white* surface representation, whereas p12 peptide in the crystallographic position is shown as *blue sticks*. PCNA residues whose amide signals significantly shift, disappear, or remain unassigned in the titration with the RecQ5 or p12 peptides are painted in *red*, *orange*, or *gray*, respectively.

and DNA damage–induced degradation of p12 (30). CRL4^{Cdt2} recognizes substrates bound to PCNA and DNA through a specialized PIP box (or PIPdegron, characterized by the Thr–Asp motif within the PIP box, which confers high affinity to PCNA, and a basic amino acid four residues downstream of the PIP box, which is required for recognition by the ligase) and triggers the degradation of several proteins, including p21 (31–33). The structure of p21 PIP box bound to PCNA suggests that an acidic patch on PCNA, centered on residues Asp^{122} and Glu^{124} on the IDCL, provides interaction for the basic residue in the PIPdegron (Fig. 8*A*), and both Asp^{122} and Glu^{124} were shown to be required for CRL4^{Cdt2} recruitment (34). Based on our X-ray structure, the basic residue of p12 degron (Lys^{15}) points away from the acidic patch on the IDCL (Figs. 4 and 8*A*). However, Lys^{15} is the last p12 C-terminal residue visible in the electron density map, and its side chain is poorly defined (Fig. 4), suggesting that it is rather flexible and may possibly reorient upon binding to CRL4^{Cdt2}, when p12 is targeted for degradation.

The PCNA binding site of p12 belongs to the broad class of PIP-like motifs

PCNA is a hub protein that physically interacts with dozens of protein partners, mostly involved in DNA transactions (7, 35). Most of the partners structurally characterized to date bind PCNA through canonical PIP boxes (36) (Fig. 8*B*, *left panel*). Notably, several X-ray crystal structures of PCNA bound to divergent PIP motifs have also been determined (37–39) (Fig. 8*B*, *right panel*). This implies that it is highly problematic, or impossible at all, to identify PCNA-interacting motifs based on sequence analysis only (21). Nonconsensus PIP motifs lacking the canonical glutamine have been described for the TLS poly-

merases η and ι, in which the glutamine residue is replaced by methionine and arginine, respectively (28) (Table 2 and Fig. 8). In both cases, an acidic residue is observed at position +5. The PIP motif of pol ι adopts a β-bend-like structure that poses the side chains of the consensus isoleucine and tyrosine and the nonconsensus leucine residues at positions +4, +7, and +8 to insert into the canonical PIP-box pocket. The PIP-like motif of PARG (KDSKITDHF (38)) shows striking similarities with the p12 motif described in this work, particularly for the lack of an aromatic residue at +7 position and the presence of an aspartate at +6 position, which creates a network of stabilizing intramolecular interactions.

A second major class of PCNA-interacting motifs named APIM (AlkB homologue 2 PCNA- interacting motif (40)) has been proposed, with consensus sequence (K/R)(F/Y/W)(L/I/V/A)(L/I/V/A)-(K/R). However, the crystal structure (41, 42) of an APIM motif (from the SWI/SNF helicase ZRANB3), bound to PCNA reveals a strong similarity between APIM and other atypical PIP-box motives in both their structures and their interaction with PCNA (Fig. 8 and Table 2). In fact, it has been proposed that the PIP motif is not a distinct entity but rather part of a broad, loosely defined class of PIP-like motives together with the RIR (Rev1-interacting region) and the MIP (Mlh1-interacting protein) motives (21). Therefore, it may be that the APIM motif is another variant of a PIP-like motif. Further crystallographic structures of APIM peptides bound to PCNA might support this hypothesis.

Surprisingly, our NMR data show that the canonical PIP-box sequence of RecQ5 helicase (QNLIRHFF) binds PCNA with lower affinity than the p12 divergent PIP motif and through a
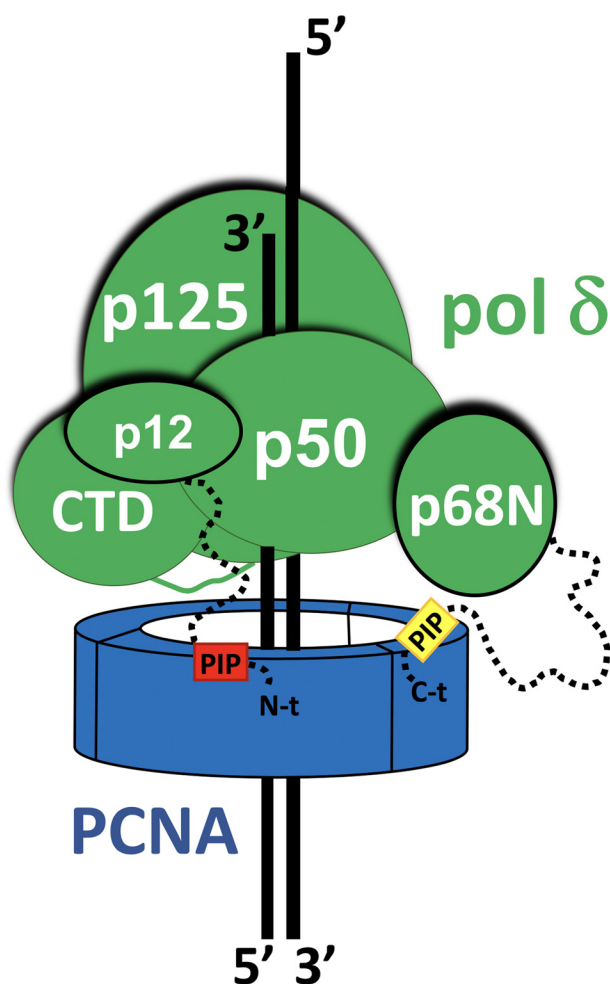
Figure 7. Possible organization of the human pol δ–PCNA complex on primer/template DNA. The N-terminal (*N-t*) and C-terminal (*C-t*) PIP motifs of p12 and p68 subunits, connected to the folded domains by disordered regions (shown as *dashed lines*), are indicated with *red* or *yellow boxes*, respectively, and binding two distinct PCNA subunits; *CTD*, p125 C-terminal Domain.

less extended surface of interaction. We propose that the low affinity of RecQ5 PIP-motif is due to the lack of the stabilizing acidic residue at +6 position. We conclude that an acidic residue at +6 position, in addition to the hydrophobic trident, is important to generate a high-affinity PIP box. This acidic residue is, however, not indispensable for binding (p68 PIP-box sequence does not have one: QVSITGFF), but at least the residue at this position should not be positively charged for a high-affinity interaction.

Experimental procedures

Protein expression and purification

Human PCNA (UniProt: P12004) was produced in *Escherichia coli* BL21(DE3) cells grown in LB medium to obtain protein with natural isotopic abundance or in isotope-enriched medium for uniform enrichment. A PCNA clone with N-terminal His$_6$ tag and HRV 3C protease cleavage site in a pET-derived plasmid was used. For NMR samples the protein was purified from the soluble fraction by Co^{2+}-affinity chromatography, cleaved by HRV 3C protease, and polished by gel-filtration chromatography (43). All columns and chromatography systems used where from GE Healthcare. Protein elution was

monitored by absorbance at 280 nm and confirmed by SDS-PAGE. The purified protein contained the extra sequence GPH- at the N terminus. The PCNA sample for crystallization was obtained by introducing two additional purification steps (44). The sample cleaved with HRV 3C protease was dialyzed against 50 mM sodium acetate, pH 5.5, 100 mM NaCl. After separation of some precipitated material, the solution was loaded on a HiTrap heparin HP column equilibrated with the same buffer. After column washing, the protein was eluted with a 0–100% gradient of 50 mM sodium acetate, pH 5.5, 2 M NaCl in 20 column volumes. The protein-containing fractions of the major peak were dialyzed against 20 mM Tris-HCl buffer, pH 7.6, 150 mM NaCl and injected into a HiTrap Chelating HP column loaded with Co^{2+} cations to remove uncleaved PCNA. The flowthrough was loaded on a HiTrap Q–Sepharose column and eluted with a 0–60% gradient of 20 mM Tris-HCl, pH 7.6, 1 M NaCl in 5 column volumes. The protein-containing fractions were concentrated and polished using a Superdex 200 26/60 column equilibrated with PBS, pH 7.0, and then exchanged into the crystallization buffer (20 mM Tris-HCl, pH 7.5, 10% glycerol, 2 mM DTT) using a PD10 column. Stock solutions in PBS or crystallization buffer were flash-frozen in liquid nitrogen and stored at −80 °C. The protein concentrations were measured by absorbance at 280 nm using the extinction coefficient calculated from the amino acid composition (15,930 M^{-1} cm^{-1}). All indicated concentrations of PCNA samples refer to protomer concentrations. The peptides were purchased as lyophilized powders from Apeptide company. The 19-residue-long N-terminal fragment of p12 (^{1}MGRKRLITDSYPV-VKRREG^{19}) was chosen to contain the PIP box plus residues that could potentially interact with the IDCL of PCNA (by comparison with the p21–PCNA structure) and that would favor solubility at pH 7.0. The peptide concentration was measured by UV absorbance using the extinction coefficient of its tyrosine residue. The 28-residue-long fragment of RecQ5 (^{952}KTSPGRSVKEEAQNLIRHFFHGRARCES^{979}) was chosen with similar criteria but elongated at the N terminus to match the length of the p15^{PAF} peptide, which also binds the inner channel of PCNA (44). The peptide does not contain any tyrosine of tryptophan, and the concentration was thus measured by UV absorbance at 205 nm (45).

NMR spectroscopy

^{1}H-^{15}N TROSY spectra were recorded at 35 °C on a Bruker Avance III 800 MHz (18.8 T) spectrometer equipped with a cryogenically cooled triple resonance z-gradient probe. A 400-μl sample of 51 μM U-[^{2}H,^{13}C,^{15}N]PCNA in PBS (10 mM phosphate, 140 mM chloride, 153 mM sodium, and 4.5 mM potassium), pH 7.0, 20 μM DSS (4,4-dimethyl-4-silapentane-1-sulfonic acid), 0.01% NaN$_3$, 1 mM DTT, and 5% ^{2}H$_2$O was placed in a 5-mm Shigemi NMR tube (without plunger), and increasing volumes of the p12 peptide stock solution at 4.9 mM were added and mixed (by capping and inverting the NMR tube), causing a 7% PCNA dilution at the last point of the titration. The peptide solution was prepared in the same buffer as the PCNA samples (except that no NaN$_3$, DSS (4,4-dimethyl-4-silapentane-1-sulfonic acid), or ^{2}H$_2$O was added). For that purpose, and to remove unwanted salts from the synthetic pep-
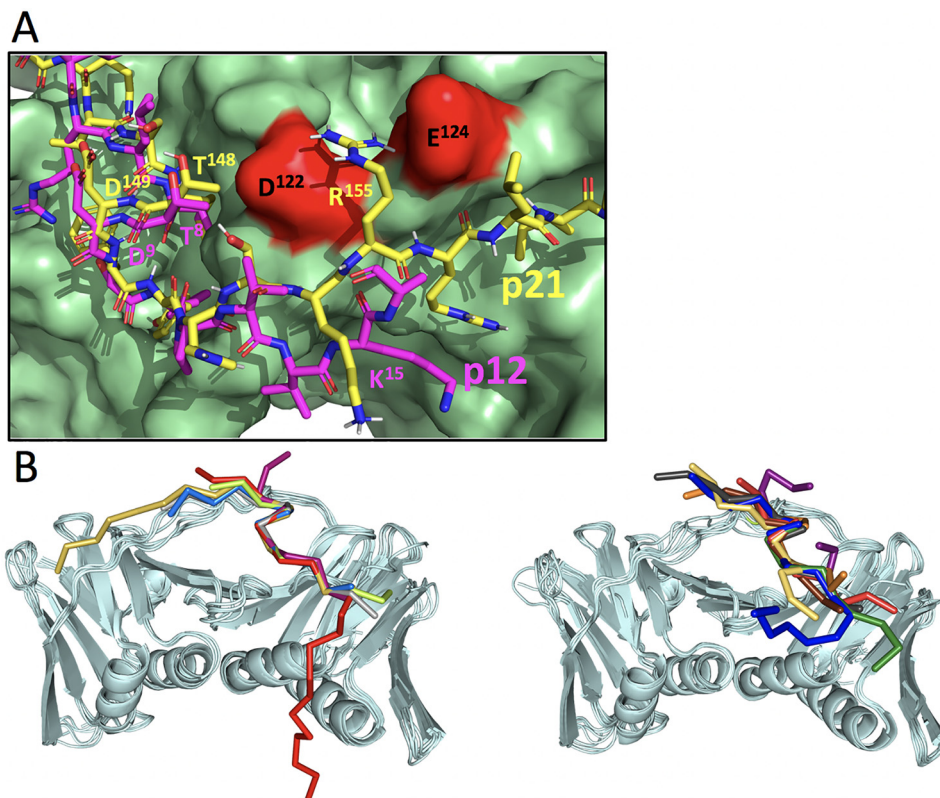
Figure 8. *A*, comparison of p21 and p12 PIP degrons interacting with PCNA. *B*, superposition of structures of canonical (*left*) and noncanonical (*right*) PCNA-interacting motifs bound to PCNA. *A*, p21–PCNA (PDB code 1AXC) (22) and p12–PCNA (PDB code 6HVO; current study) structures are aligned. p21 and p12 peptides are shown as *yellow* and *magenta sticks*, respectively. PCNA is shown as a *green surface*. The residues making up the acidic patch in the IDCL are colored *red*. *B*, *left panel*, the PCNA protomers are represented by *ribbons*, and the peptides are represented by their Cα traces. The color code is as follows: p21, *yellow* (PDB code 1AXC) (22); p15^{PAF}, *red* (PDB code 4D2G) (44); FEN-1, *blue* (PDB code 1U7B) (20); p68, *green* (PDB code 1U76) (20); ZRANB3-PIP, *purple* (PDB code 5MLO) (42); DVC1, *gray* (PDB code 5IY4) (53). *B*, *right panel*, the color code is as follows: PARG, *gray* (PDB code 5MAV) (38); ZRANB3-APIM, *brown* (PDB code 5MLW) (41); pol η, *blue* (PDB code 2ZVK) (37); pol ι, *purple* (PDB code 2ZVM) (37); pol κ, *yellow* (PDB code 2ZVL) (37); RNH2B, *green* (PDB code 3P87) (54); TRAIP, *red* (PDB code 4ZTD) (29); and p12, *orange* (PDB code 6HVO).

Table 2

Sequence alignment of PCNA-interacting protein fragments in crystal structures bound to PCNA. Consensus residues are highlighted. The residues shown in the alignment are those observed in the crystal structure and do not include terminal disordered residues present in the peptides.

Protein	Sequence
p21	RQTSMTDFYHSKRRLIFS
p68	KANRQVSLTGFFQRK
p15	GNPVCVRPTPKWQKGIGEFFRL
FEN1	TQGRLDDFFKVTG
ZRANB3(PIP)	KQHDIRSFFVP
p12	RKRLITDSYPVVK
Pol ι	KKGLIDYYLMPSL
Pol η	GMQTLESFFKPLT
PARG	KDSKITDHFMRL
Pol κ	FKHTLDIFFKFLT
ZRANB3(APIM)	ASKHGSDTRFLVKK
RNH2B	DKSGMKSIDTFF

between the backbone amide ^{1}H and ^{15}N chemical shifts in the free and bound states (43), and the estimated error in the calculated CSP is ±0.005 ppm. The fitting of the CSP changes (for those residues with CSPs larger than the average plus one standard deviation) was performed using a single-site binding model, and the reported K_d is the average over all selected residues with the standard deviation as an estimate of its uncertainty. The NMR titration of PCNA with the peptide from RecQ5 was done in the same conditions as p12 except that the peptide stock solution was 3.5 mM and that the intermediate titration points were monitored with ^{1}H-^{15}N HMQC spectra using 124 indirect points and a total duration of 10.6 h. The assignment coverage was 83% of nonproline residues).

Isothermal calorimetry

For ITC measurements, we employed an ITC200 calorimeter with 190 μM PCNA in the cell. The PCNA protein solution (dialyzed against PBS, pH 7.0, 2 mM TCEP) was titrated with a 6 mM stock solution of p12 prepared by dissolving the lyophilized material in the dialysis buffer and adjusting the pH to 7.0 with NaOH. A sequence of variable injection volumes was designed based on simulations (one injection of 0.3 μl, five injections of 0.5 μl, five injections of 1.0 μl, seven injections of 2.0 μl, and 7 injections of 2.5 μl). The heat produced by the binding reaction was obtained as the difference between the heat of reaction and

tide, the lyophilized powder was dissolved in PBS, pH 7.0, and passed through a PD-10 Minitrap G25 column. BEST-^{1}H-^{15}N-TROSY spectra were measured with 256 indirect points for a total duration of 21.3 h. The p12–PCNA sample remained clear during the 6-day-long titration. The titration with the peptide allowed for an extensive transfer of NMR signal assignments from the free PCNA to the p12-bound PCNA spectra (with a coverage of 73% of nonproline residues). The CSPs caused by the peptide were computed as the weighted average distance

the corresponding heat of dilution, as obtained from an independent titration of the peptides into the buffer. The binding isotherm was analyzed by nonlinear least-squares fitting of the experimental data to a model assuming a single set of equivalent sites (46), using Microcal Origin (OriginLab) and in-house developed software.

p12–PCNA complex crystallization and structure determination

Stocks of PCNA and p12 peptide solutions were mixed to final concentrations of 0.4 and 0.5 mM, respectively (1:1.2 protein monomer:peptide), and incubated at room temperature for 30 min before screening crystallization conditions using the hanging-drop vapor-diffusion method. Best diffracting co-crystals grew within 2 days at 18 °C in droplets obtained by mixing 1 μl of the complex solution and 1 μl of a solution containing 24% PEG 3350 in 0.2 M lithium sulfate buffer, pH 6.5. The crystals were transferred to precipitant solution supplemented with 20% PEG 400 and flash frozen in liquid nitrogen. The best crystals from the p12–PCNA complex diffracted at 2.1 Å resolution on the ALBA Beamline XALOC (Barcelona, Spain) and belonged to $P2_12_12_1$ space group. XDS (47) and the CCP4i suite (48) were used for data processing. Molecular replacement was used to place one human PCNA trimer (PDB code 1VYM) (23) in the asymmetric unit. Several cycles of refinement using REFMAC5 (49) and model building using COOT (50) were carried out before placing the three p12 chains into the $F_o - F_c$ electron density map. Data collection and refinement statistics are listed in Table 1. All figures with molecular models were prepared using PyMOL.

Author contributions—A. G.-M., A. I. d. O., M. R.-M., J. M.-C., N. M., I. L., A. L. R., and F. J. B. formal analysis; A. G.-M., A. I. d. O., M. R.-M., J. M.-C., N. M., I. L., F. J. B., and A. D. B. investigation; I. L., F. J. B., and A. D. B. conceptualization; S. O., F. J. B., and A. D. B. supervision; S. O., F. J. B., and A. D. B. writing-original draft; F. J. B. funding acquisition; A. D. B. validation; A. D. B. project administration.

References

1. Hubscher, U., Maga, G., and Spadari, S. (2002) Eukaryotic DNA polymerases. *Annu. Rev. Biochem.* **71,** 133–163 CrossRef Medline
2. Lee, M., Wang, X., Zhang, S., Zhang, Z., and Lee, E. Y. C. (2017) Regulation and modulation of human DNA polymerase δ activity and function. *Genes (Basel)* **8,** E190 CrossRef Medline
3. Zhang, S., Zhou, Y., Trusa, S., Meng, X., Lee, E. Y., and Lee, M. Y. (2007) A novel DNA damage response: rapid degradation of the p12 subunit of DNA polymerase δ. *J. Biol. Chem.* **282,** 15330–15340 CrossRef Medline
4. Meng, X., Zhou, Y., Zhang, S., Lee, E. Y., Frick, D. N., and Lee, M. Y. (2009) DNA damage alters DNA polymerase δ to a form that exhibits increased discrimination against modified template bases and mismatched primers. *Nucleic Acids Res.* **37,** 647–657 Medline
5. Meng, X., Zhou, Y., Lee, E. Y., Lee, M. Y., and Frick, D. N. (2010) The p12 subunit of human polymerase δ modulates the rate and fidelity of DNA synthesis. *Biochemistry* **49,** 3545–3554 CrossRef Medline
6. Tan, C. K., Castillo, C., So, A. G., and Downey, K. M. (1986) An auxiliary protein for DNA polymerase-δ from fetal calf thymus. *J. Biol. Chem.* **261,** 12310–12316 Medline
7. Choe, K. N., and Moldovan, G. L. (2017) Forging ahead through darkness: PCNA, still the principal conductor at the replication fork. *Mol. Cell* **65,** 380–392 CrossRef Medline
8. Prelich, G., Kostura, M., Marshak, D. R., Mathews, M. B., and Stillman, B. (1987) The cell-cycle regulated proliferating cell nuclear antigen is required for SV40 DNA replication *in vitro*. *Nature* **326,** 471–475 CrossRef Medline
9. Lee, M. Y., Tan, C. K., Downey, K. M., and So, A. G. (1984) Further studies on calf thymus DNA polymerase δ purified to homogeneity by a new procedure. *Biochemistry* **23,** 1906–1913 CrossRef Medline
10. Li, H., Xie, B., Zhou, Y., Rahmeh, A., Trusa, S., Zhang, S., Gao, Y., Lee, E. Y., and Lee, M. Y. (2006) Functional roles of p12, the fourth subunit of human DNA polymerase δ. *J. Biol. Chem.* **281,** 14748–14755 CrossRef Medline
11. Xie, B., Mazloum, N., Liu, L., Rahmeh, A., Li, H., and Lee, M. Y. (2002) Reconstitution and characterization of the human DNA polymerase δ four-subunit holoenzyme. *Biochemistry* **41,** 13133–13142 CrossRef Medline
12. Baranovskiy, A. G., Babayeva, N. D., Liston, V. G., Rogozin, I. B., Koonin, E. V., Pavlov, Y. I., Vassylyev, D. G., and Tahirov, T. H. (2008) X-ray structure of the complex of regulatory subunits of human DNA polymerase δ. *Cell Cycle* **7,** 3026–3036 CrossRef Medline
13. Tahirov, T. H. (2012) Structure and function of eukaryotic DNA polymerase δ. *Subcell. Biochem.* **62,** 217–236 CrossRef Medline
14. Zhang, S. J., Zeng, X. R., Zhang, P., Toomey, N. L., Chuang, R. Y., Chang, L. S., and Lee, M. Y. (1995) A conserved region in the amino terminus of DNA polymerase δ is involved in proliferating cell nuclear antigen binding. *J. Biol. Chem.* **270,** 7988–7992 CrossRef Medline
15. Zhang, P., Mo, J. Y., Perez, A., Leon, A., Liu, L., Mazloum, N., Xu, H., and Lee, M. Y. (1999) Direct interaction of proliferating cell nuclear antigen with the p125 catalytic subunit of mammalian DNA polymerase δ. *J. Biol. Chem.* **274,** 26647–26653 CrossRef Medline
16. Zhou, Y., Meng, X., Zhang, S., Lee, E. Y., and Lee, M. Y. (2012) Characterization of human DNA polymerase δ and its subassemblies reconstituted by expression in the MultiBac system. *PLoS One* **7,** e39156 CrossRef Medline
17. Wang, Y., Zhang, Q., Chen, H., Li, X., Mai, W., Chen, K., Zhang, S., Lee, E. Y., Lee, M. Y., and Zhou, Y. (2011) P50, the small subunit of DNA polymerase δ, is required for mediation of the interaction of polymerase δ subassemblies with PCNA. *PLoS One* **6,** e27092 CrossRef Medline
18. Mo, J., Liu, L., Leon, A., Mazloum, N., and Lee, M. Y. (2000) Evidence that DNA polymerase δ isolated by immunoaffinity chromatography exhibits high-molecular weight characteristics and is associated with the KIAA0039 protein and RPA. *Biochemistry* **39,** 7245–7254 CrossRef Medline
19. Rahmeh, A. A., Zhou, Y., Xie, B., Li, H., Lee, E. Y., and Lee, M. Y. (2012) Phosphorylation of the p68 subunit of Pol δ acts as a molecular switch to regulate its interaction with PCNA. *Biochemistry* **51,** 416–424 CrossRef Medline
20. Bruning, J. B., and Shamoo, Y. (2004) Structural and thermodynamic analysis of human PCNA with peptides derived from DNA polymerase-δ p66 subunit and flap endonuclease-1. *Structure* **12,** 2209–2219 CrossRef Medline
21. Boehm, E. M., and Washington, M. T. (2016) R.I.P. to the PIP: PCNA-binding motif no longer considered specific: PIP motifs and other related sequences are not distinct entities and can bind multiple proteins involved in genome maintenance. *Bioessays* **38,** 1117–1122 CrossRef Medline
22. Gulbis, J. M., Kelman, Z., Hurwitz, J., O'Donnell, M., and Kuriyan, J. (1996) Structure of the C-terminal region of p21(WAF1/CIP1) complexed with human PCNA. *Cell* **87,** 297–306 CrossRef Medline
23. Kontopidis, G., Wu, S. Y., Zheleva, D. I., Taylor, P., McInnes, C., Lane, D. P., Fischer, P. M., and Walkinshaw, M. D. (2005) Structural and biochemical studies of human proliferating cell nuclear antigen complexes provide a rationale for cyclin association and inhibitor design. *Proc. Natl. Acad. Sci. U.S.A.* **102,** 1871–1876 CrossRef Medline

ASBMB

J. Biol. Chem. (2019) 294(11) 3947–3956 **3955**

24. Urban, V., Dobrovolna, J., Hühn, D., Fryzelkova, J., Bartek, J., and Janscak, P. (2016) RECQ5 helicase promotes resolution of conflicts between replication and transcription in human cells. *J. Cell Biol.* **214,** 401–415 CrossRef Medline

25. Kanagaraj, R., Saydam, N., Garcia, P. L., Zheng, L., and Janscak, P. (2006) Human RECQ5β helicase promotes strand exchange on synthetic DNA structures resembling a stalled replication fork. *Nucleic Acids Res.* **34,** 5217–5231 CrossRef Medline

26. Hedglin, M., Pandey, B., and Benkovic, S. J. (2016) Characterization of human translesion DNA synthesis across a UV-induced DNA lesion. *Elife* **5**, pii: e19788 CrossRef Medline

27. Xu, H., Zhang, P., Liu, L., and Lee, M. Y. (2001) A novel PCNA-binding motif identified by the panning of a random peptide display library. *Biochemistry* **40,** 4512–4520 CrossRef Medline

28. Nishida, H., Mayanagi, K., Kiyonari, S., Sato, Y., Oyama, T., Ishino, Y., and Morikawa, K. (2009) Structural determinant for switching between the polymerase and exonuclease modes in the PCNA-replicative DNA polymerase complex. *Proc. Natl. Acad. Sci. U.S.A.* **106,** 20693–20698 CrossRef Medline

29. Hoffmann, S., Smedegaard, S., Nakamura, K., Mortuza, G. B., Räschle, M., Ibañez de Opakua, A., Oka, Y., Feng, Y., Blanco, F. J., Mann, M., Montoya, G., Groth, A., Bekker-Jensen, S., and Mailand, N. (2016) TRAIP is a PCNA-binding ubiquitin ligase that protects genome stability after replication stress. *J. Cell Biol.* **212,** 63–75 CrossRef Medline

30. Zhang, S., Zhao, H., Darzynkiewicz, Z., Zhou, P., Zhang, Z., Lee, E. Y., and Lee, M. Y. (2013) A novel function of CRL4(Cdt2): regulation of the subunit structure of DNA polymerase δ in response to DNA damage and during the S phase. *J. Biol. Chem.* **288,** 29550–29561 CrossRef Medline

31. Havens, C. G., and Walter, J. C. (2009) Docking of a specialized PIP box onto chromatin-bound PCNA creates a degron for the ubiquitin ligase CRL4Cdt2. *Mol. Cell* **35,** 93–104 CrossRef Medline

32. Abbas, T., Sivaprasad, U., Terai, K., Amador, V., Pagano, M., and Dutta, A. (2008) PCNA-dependent regulation of p21 ubiquitylation and degradation via the CRL4Cdt2 ubiquitin ligase complex. *Genes Dev.* **22,** 2496–2506 CrossRef Medline

33. Michishita, M., Morimoto, A., Ishii, T., Komori, H., Shiomi, Y., Higuchi, Y., and Nishitani, H. (2011) Positively charged residues located downstream of PIP box, together with TD amino acids within PIP box, are important for CRL4(Cdt2)- mediated proteolysis. *Genes Cells* **16,** 12–22 CrossRef Medline

34. Havens, C. G., Shobnam, N., Guarino, E., Centore, R. C., Zou, L., Kearsey, S. E., and Walter, J. C. (2012) Direct role for proliferating cell nuclear antigen in substrate recognition by the E3 ubiquitin ligase CRL4Cdt2. *J. Biol. Chem.* **287,** 11410–11421 CrossRef Medline

35. Moldovan, G. L., Pfander, B., and Jentsch, S. (2007) PCNA, the maestro of the replication fork. *Cell* **129,** 665–679 CrossRef Medline

36. De Biasio, A., and Blanco, F. J. (2013) Proliferating cell nuclear antigen structure and interactions: too many partners for one dancer? *Adv. Protein Chem. Struct. Biol.* **91,** 1–36 CrossRef Medline

37. Hishiki, A., Hashimoto, H., Hanafusa, T., Kamei, K., Ohashi, E., Shimizu, T., Ohmori, H., and Sato, M. (2009) Structural basis for novel interactions between human translesion synthesis polymerases and proliferating cell nuclear antigen. *J. Biol. Chem.* **284,** 10552–10560 CrossRef Medline

38. Kaufmann, T., Grishkovskaya, I., Polyansky, A. A., Kostrhon, S., Kukolj, E., Olek, K. M., Herbert, S., Beltzung, E., Mechtler, K., Peterbauer, T., Gotzmann, J., Zhang, L., Hartl, M., Zagrovic, B., Elsayad, K., *et al.* (2017) A novel non-canonical PIP-box mediates PARG interaction with PCNA. *Nucleic Acids Res.* **45,** 9741–9759 CrossRef Medline

39. Armstrong, A. A., Mohideen, F., and Lima, C. D. (2012) Recognition of SUMO-modified PCNA requires tandem receptor motifs in Srs2. *Nature* **483,** 59–63 CrossRef Medline

40. Olaisen, C., Kvitvang, H. F. N., Lee, S., Almaas, E., Bruheim, P., Drabløs, F., and Otterlei, M. (2018) The role of PCNA as a scaffold protein in cellular signaling is functionally conserved between yeast and humans. *FEBS Open Bio.* **8,** 1135–1145 CrossRef Medline

41. Hara, K., Uchida, M., Tagata, R., Yokoyama, H., Ishikawa, Y., Hishiki, A., and Hashimoto, H. (2018) Structure of proliferating cell nuclear antigen (PCNA) bound to an APIM peptide reveals the universality of PCNA interaction. *Acta Crystallogr. F Struct. Biol. Commun.* **74,** 214–221 CrossRef Medline

42. Sebesta, M., Cooper, C. D. O., Ariza, A., Carnie, C. J., and Ahel, D. (2017) Structural insights into the function of ZRANB3 in replication stress response. *Nat. Commun.* **8,** 15847 CrossRef Medline

43. De Biasio, A., Campos-Olivas, R., Sanchez, R., Lopez-Alonso, J. P., Pantoja-Uceda, D., Merino, N., Villate, M., Martin-Garcia, J. M., Castillo, F., Luque, I., and Blanco, F. J. (2012) Proliferating cell nuclear antigen (PCNA) interactions in solution studied by NMR. *PLoS One* **7**, e48390 CrossRef Medline

44. De Biasio, A., de Opakua, A. I., Mortuza, G. B., Molina, R., Cordeiro, T. N., Castillo, F., Villate, M., Merino, N., Delgado, S., Gil-Cartón, D., Luque, I., Diercks, T., Bernadó, P., Montoya, G., and Blanco, F. J. (2015) Structure of p15(PAF)-PCNA complex and implications for clamp sliding during DNA replication and repair. *Nat. Commun.* **6,** 6439 CrossRef Medline

45. Anthis, N. J., and Clore, G. M. (2013) Sequence-specific determination of protein and peptide concentrations by absorbance at 205 nm. *Protein Sci.* **22,** 851–858 CrossRef Medline

46. Palacios, A., Muñoz, I. G., Pantoja-Uceda, D., Marcaida, M. J., Torres, D., Martín-García, J. M., Luque, I., Montoya, G., and Blanco, F. J. (2008) Molecular basis of histone H3K4me3 recognition by ING4. *J. Biol. Chem.* **283,** 15956–15964 CrossRef Medline

47. Kabsch, W. (2010) Integration, scaling, space-group assignment and post-refinement. *Acta Crystallogr. D Biol. Crystallogr.* **66,** 133–144 CrossRef Medline

48. Winn, M. D., Ballard, C. C., Cowtan, K. D., Dodson, E. J., Emsley, P., Evans, P. R., Keegan, R. M., Krissinel, E. B., Leslie, A. G., McCoy, A., McNicholas, S. J., Murshudov, G. N., Pannu, N. S., Potterton, E. A., Powell, H. R., *et al.* (2011) Overview of the CCP4 suite and current developments. *Acta Crystallogr. D Biol. Crystallogr.* **67,** 235–242 CrossRef Medline

49. Murshudov, G. N., Skubák, P., Lebedev, A. A., Pannu, N. S., Steiner, R. A., Nicholls, R. A., Winn, M. D., Long, F., and Vagin, A. A. (2011) REFMAC5 for the refinement of macromolecular crystal structures. *Acta Crystallogr. D Biol. Crystallogr.* **67,** 355–367 CrossRef Medline

50. Emsley, P., Lohkamp, B., Scott, W. G., and Cowtan, K. (2010) Features and development of Coot. *Acta Crystallogr. D Biol. Crystallogr.* **66,** 486–501 CrossRef Medline

51. Ishida, T., and Kinoshita, K. (2007) PrDOS: prediction of disordered protein regions from amino acid sequence. *Nucleic Acids Res.* **35,** W460–W464 CrossRef Medline

52. Drozdetskiy, A., Cole, C., Procter, J., and Barton, G. J. (2015) JPred4: a protein secondary structure prediction server. *Nucleic Acids Res.* **43,** W389–W394 CrossRef Medline

53. Wang, Y., Xu, M., and Jiang, T. (2016) Crystal structure of human PCNA in complex with the PIP box of DVC1. *Biochem. Biophys. Res. Commun.* **474,** 264–270 CrossRef Medline

54. Bubeck, D., Reijns, M. A., Graham, S. C., Astell, K. R., Jones, E. Y., and Jackson, A. P. (2011) PCNA directs type 2 RNase H activity on DNA replication and repair substrates. *Nucleic Acids Res.* **39,** 3652–3666 CrossRef Medline

ASBMB

The p12 subunit of human polymerase δ uses an atypical PIP box for molecular recognition of proliferating cell nuclear antigen (PCNA)

Amaia Gonzalez-Magaña, Alain Ibáñez de Opakua, Miguel Romano-Moreno, Javier Murciano-Calles, Nekane Merino, Irene Luque, Adriana L. Rojas, Silvia Onesti, Francisco J. Blanco and Alfredo De Biasio

Access the most updated version of this article at doi: 10.1074/jbc.RA118.006391

Alerts:
- When this article is cited
- When a correction for this article is posted

Click here to choose from all of JBC's e-mail alerts

This article cites 54 references, 14 of which can be accessed free at
http://www.jbc.org/content/294/11/3947.full.html#ref-list-1